Theoretical fluxes of gamma rays from the Martian surface

Article *in* Journal of Geophysical Research Atmospheres · December 2006

DOI: 10.1029/2005JE002655

5 authors, including:

Kyeong J Kim
Korea Institute of Geoscience and Mineral Resources
145 PUBLICATIONS **1,110** CITATIONS
SEE PROFILE

Robert C Reedy
Planetary Science Institute
522 PUBLICATIONS **8,036** CITATIONS
SEE PROFILE

William V. Boynton
The University of Arizona
795 PUBLICATIONS **14,596** CITATIONS
SEE PROFILE

Theoretical fluxes of gamma rays from the Martian surface

Kyeong J. Kim,[1,2] Darrell M. Drake,[3] Robert C. Reedy,[1] Remo M. S. Williams,[4] and William V. Boynton[4]

Received 30 November 2005; revised 5 May 2006; accepted 25 May 2006; published 14 December 2006.

[1] Theoretical fluxes of gamma rays escaping the surface of Mars were calculated. These and other calculated fluxes are needed to model the counting rates in the Mars Odyssey gamma ray spectrometer that are used to determine elemental compositions and other results using these measurements. Cross sections for the formation of gamma rays by both thermal and fast neutrons were compiled and evaluated. These evaluated cross sections were used with neutron fluxes calculated with the Monte Carlo N Particle Extended (MCNPX) code to get gamma ray production rates as a function of depth in the Martian surface. The fluxes of these gamma rays as a function of angle at the Martian surface were then calculated using gamma ray attenuation coefficients.

Citation: Kim, K. J., D. M. Drake, R. C. Reedy, R. M. S. Williams, and W. V. Boynton (2006), Theoretical fluxes of gamma rays from the Martian surface, *J. Geophys. Res.*, *111*, E03S09, doi:10.1029/2005JE002655 [printed *112*(E3), 2007].

1. Introduction

[2] The 2001 Mars Odyssey spacecraft has been in a circular, nearly polar orbit around Mars since 24 October 2001 [*Saunders et al.*, 2004]. The gamma ray spectrometer suite of instruments [*Boynton et al.*, 2004] is one of three scientific instruments onboard the spacecraft [*Saunders et al.*, 2004]. The gamma ray spectrometer suite includes an instrument to detect gamma rays, the gamma ray spectrometer (GRS), and two instruments to detect neutrons, the neutron spectrometer (NS) and the high-energy neutron detector (HEND). Data from these instruments are used to map the concentrations of elements in the top few 10s of cm of the Mars surface. Following its deployment on a 6 m long boom, the GRS has been accumulating high-quality gamma ray spectra since 6 June 2002.

[3] Details on the gamma ray spectrometer suite of instruments are given by *Boynton et al.* [2004]. The details of the procedures on how the measured gamma ray spectra and data are converted to elemental abundances are given by W. V. Boynton et al. (Concentration of H, Si, Cl, K, Fe, and Th in the low-latitude and midlatitude regions of Mars, submitted to *Journal of Geophysical Research*, 2006, hereinafter referred to as Boynton et al., submitted manuscript, 2006). In calculating the expected gamma ray count rate in the GRS at each spacecraft location, which is needed to obtain elemental abundances, it is necessary to integrate the signal expected over all angles to the entire solid surface within view of this location. For the GRS, this integration is done by dividing the Martian surface into $0.5^\circ \times 0.5^\circ$ cells on the surface. At the location of the spacecraft for each 20 s duration gamma ray spectrum, the angle from the spacecraft to each $0.5^\circ \times 0.5^\circ$ cell in a 17° radius footprint (from which about 99% of the gamma rays at the GRS are emitted) is calculated. From this angle, the appropriate flux from each cell is found by interpolation. The total flux at the spacecraft is calculated by taking the surface flux from each cell, calculating the attenuation in the atmosphere (which varies with time and surface position), and summing over all cells in the footprint. The angular flux of gamma rays escaping the surface depends strongly on the composition of the surface, especially its hydrogen content, and the atmospheric thickness [*Masarik and Reedy*, 1996]. Reported here are details on the calculation of these fluxes, especially the nuclear data and codes used.

[4] The main sources of the gamma ray lines used for elemental work are nuclear reactions with all elements induced by fast (energies above $\sim$1 MeV) and thermal ($\sim$0.02 eV) neutrons and the decay of the naturally occurring long-lived radionuclides ^{40}K, ^{232}Th, ^{238}U, and their daughters. The neutrons that produce gamma rays are made by high-energy (GeV) galactic cosmic ray (GCR) particles. We calculate that $\sim$15 neutrons are made on Mars per GCR particle.

[5] The first detailed set of calculated planetary gamma ray fluxes was reported by *Reedy et al.* [1973] for the Moon. These calculations were improved using better nuclear data by *Reedy* [1978]. These papers summarized the basic approaches of such calculations and gave fluxes at the lunar surface for a range of lunar compositions. For example, *Reedy et al.* [1973] discussed calculated fluxes and presented a simple formula for the fluxes of gamma rays from the decay of naturally occurring radionuclides. *Reedy* [1978] compiled sets of nuclear data for the gamma rays made by reactions of fast and thermal neutrons, and these nuclear data have been used by most later workers [e.g., *Dagge et al.*, 1991; *Masarik and Reedy*, 1996]. *Reedy*

[1]Institute of Meteoritics, University of New Mexico, Albuquerque, New Mexico, USA.
[2]Now at Lunar and Planetary Laboratory, University of Arizona, Tucson, Arizona, USA.
[3]TechSource, Santa Fe, New Mexico, USA.
[4]Lunar and Planetary Laboratory, University of Arizona, Tucson, Arizona, USA.

0148-0227/06/2005JE002655

[1978] discussed the effect of composition on the production of gamma rays made by neutron capture reactions. The fluxes of fast neutrons and of the gamma rays that they produce are also affected by the bulk composition, with heavier elements (such as Ti and Fe) producing more fast neutrons per cosmic ray particle than lighter elements (such as Mg and Si) [*Masarik and Reedy*, 1994].

[6] These and other calculations have been used to determine elemental abundances from gamma ray spectra measured by Apollo [e.g., *Bielefeld et al.*, 1976] and Lunar Prospector [e.g., *Prettyman et al.*, 2002, 2006] at the Moon and by NEAR-Shoemaker [*Evans et al.*, 2001] at the asteroid 433 Eros. For the Moon and Eros, the only parameter that needed to be considered was the composition of the surface. However, Mars is more complicated, having an atmosphere that varies in thickness both with time and location and surfaces with wide ranges in the abundances of H and C, two elements that cause major variations in neutron and gamma ray fluxes [e.g., *Evans and Squyres*, 1987; *Masarik and Reedy*, 1996]. To get the best possible calculated fluxes, we use the most recent nuclear data for gamma−ray production and codes for calculating neutron fluxes. We do not present any details for the naturally occurring radionuclides, as the basic data (half-lives and gamma ray intensities) and procedures have not changed significantly from those used by *Reedy et al.* [1973] and *Reedy* [1978].

2. Nuclear Data

[7] Two types of nuclear data are needed for the gamma rays used to determine most elemental abundances: those for the capture of thermal neutrons and those for reactions induced by fast neutrons. Both types of neutrons are produced by GCR particles, but they differ because of the nature of their transport and interactions [cf. *Masarik and Reedy*, 1996]. The elements that can affect them are often in common, such as H and Fe, but some elements only affect one class of neutrons, such as Cl with thermal neutrons. The nature of the nuclear data is also different, with usually only one cross section for the production by thermal neutrons but with cross sections for a range of energies for fast neutrons.

[8] The gamma rays made by thermal and fast neutrons have been often presented [e.g., *Reedy*, 1978; *Masarik and Reedy*, 1996]. Many of the gamma rays presented here have been used previously for elemental analyses. Some gamma rays are only briefly mentioned here because they are readily made in the structural material, such as Mg, Ti, and Ge, in the GRS. Gamma rays from these elements are often used as a measure of the fluxes of thermal or fast neutrons at the GRS.

2.1. Neutron Capture Reactions

[9] All the elements being mapped with neutron capture gamma rays have neutron capture cross sections that vary with neutron energy almost exactly inversely with the neutron's speed. For these elements, only a cross section measured at the accepted thermal energy (0.025 eV) is needed, as the fraction of captures that occur at other energies is the same for all of the elements considered here.

[10] The data for the production of gamma rays by thermal neutrons were adopted from two sources. One set was intensities per neutron capture that was based on an evaluation of measurements in the literature [*Reedy and Frankle*, 2002; *Frankle et al.*, 2001]. For most elements with Z (atomic number) up to 30 (almost all elements of interest in Mars), the data for neutron capture gamma rays in the literature appear to be of high quality. These data are complete (all sums are almost 100%), and often two or more sets of measurements are in good agreement [*Reedy and Frankle*, 2002]. The few elements with $Z \leq 30$ with slightly lower-quality data sets include Cr, Mn, Co, and Zn. For $Z > 30$, there are usually so many gamma rays that very few elements have had all of their gamma rays measured, thus the data often are not of good quality.

[11] The lack of good neutron capture data for many elements was well known to those who use thermal and cold neutrons from reactors to determine elemental compositions using prompt gamma ray activation analysis (PGAA). To improve the database for PGAA, the International Atomic Energy Agency (IAEA) initiated in 1999 an international project of new measurements, compilations, and evaluations [*Molnar et al.*, 2000; *Firestone et al.*, 2003]. The results of this IAEA project on PGAA are available online (http://www-nds.iaea.org/pgaa/) and in a technical document (Choi et al., manuscript in preparation, 2006). The IAEA results are given as the thermal neutron cross section for making each gamma ray. Total neutron capture cross sections for these elements are well known, so one can readily convert the cross section for making a gamma ray to its intensity per capture, or vice versa. The results of the IAEA work are generally consistent with the evaluations of *Reedy and Frankle* [2002] and were adopted here. The IAEA cross sections for gamma rays from Al are too low (F. B. Firestone, personal communication, 2004), so the results of *Reedy and Frankle* [2002] were adopted. The IAEA results for Zr (a minor element in the large amounts of magnesium around the GRS) strongly disagree with the existing data, but no gamma rays from Zr have yet to be observed in the GRS spectra.

[12] The neutron capture gamma rays and their adopted thermal cross sections and intensities per 100 captures in the element of interest are given in Table 1. All of the gamma rays are prompt except the 1294 keV gamma ray from the decay of the 110 minute radionuclide ^{41}Ar made in the Martian atmosphere by the ^{40}Ar(n,γ)^{41}Ar reaction. All energies except for the Ar gamma ray at 1294 keV and all cross sections except for the Al gamma ray at 7724 keV and the Ar gamma ray at 1294 keV are from the IAEA PGAA work. These energies are within 0.2 keV of those of *Reedy and Frankle* [2002] except the 4745 keV gamma ray from Ar and the 8884 keV gamma ray from Cr. The intensity of the Al gamma ray is from *Reedy and Frankle* [2002]. The energy and intensity of the 1294 keV gamma ray were taken from published data for the decay of ^{41}Ar. Included in Table 1 are the gamma rays routinely used (H, Si, Cl, and Fe) or that could be used for elemental abundances (C, N, Na, Al, S, Ar, Cr, Mn, and Ni) and a few neutron capture gamma rays from the material around the GRS (Mg, Ti, and Ge). The energies are usually known to better than 0.1 keV, except the 1186.8 and 4745.3 keV prompt gamma rays from Ar, which are reported by the IAEA PGAA team to be known to only 0.3 and 0.8 keV, respectively. The adopted intensities are usually in good agreement with those of

Table 1. Gamma Rays From the Capture of Thermal Neutrons, the Cross Sections for Their Production, and the Number of Each Gamma Ray per 100 Captures of Thermal Neutrons in That Element

Isotope	Energy, keV	Cross Section, b	Intensity/(100 Captures)
^{1}H	2223.2	0.333	100.
^{12}C	4945.3	0.0026	68.
^{14}N	1884.8	0.0147	18.5
^{23}Na	3587.5	0.0596	11.
^{23}Na	3981.5	0.0677	13.
^{24}Mg	3916.8	0.032	48.
^{27}Al	7724.0	0.061	27.
^{28}Si	3539.0	0.119	69.
^{28}Si	4933.9	0.112	65.
^{32}S	2379.7	0.208	39.
^{32}S	5420.6	0.308	58.
^{35}Cl	1164.9	8.91	27.
^{35}Cl	1951.1	6.33	19.
^{35}Cl	1959.3	4.10	12.
^{35}Cl	6110.8	6.59	20.
^{35}Cl	7414.0	3.29	10.
^{35}Cl	7790.3	2.66	8.
^{40}Ar	1186.8	0.34	50.
^{40}Ar	1293.6	0.67	99.
^{40}Ar	4745.3	0.36	53.
^{40}Ca	1942.7	0.35	82.
^{48}Ti	1381.7	5.18	85.
^{48}Ti	6760.1	2.97	49.
^{53}Cr	8884.4	0.78	25.
^{55}Mn	7243.5	1.36	10.
^{56}Fe	5920.4	0.225	8.8
^{56}Fe	6018.5	0.227	8.9
^{56}Fe	7631.1	0.653	25.5
^{56}Fe	7645.5	0.549	21.4
^{54}Fe	9297.7	0.075	2.9
^{58}Ni	8998.4	1.49	34.
^{73}Ge	595.8	1.10	48.
^{73}Ge	608.4	0.25	11.
^{73}Ge	1204.2	0.141	6.1

Reedy and Frankle [2002], and the ratios of intensities are within a few percent of each other. The cross sections (or intensities) are probably good to a few per cent, except the two prompt gamma rays from Ar, which are estimated by the IAEA PGAA team to have uncertainties of ~10%. These energies are within a keV of those of *Reedy* [1978], with the largest difference being the 5420.6 keV gamma ray for S. The intensities are not very different from those of *Reedy* [1978].

[13] Other neutron capture gamma rays that have been considered for use to get elemental abundances in the Martian surface but that have not yet been observed in the GRS spectra [cf. *Evans et al.*, 2006] include the most intense gamma rays (with their production cross sections in barns, with 1 b = 10^{-24} cm^2) for neutron capture reactions with Br at 776.5 keV (0.99 b), with ^{149}Sm at 334.0 keV (4790 b), and with ^{157}Gd at 181.9 keV (7200 b) and 6750.1 keV (965 b). Some gamma rays are not listed because of interferences from stronger peaks, such as the Ca gamma ray at 6419.6 keV, which is buried by a large neutron capture gamma ray from Ti at 6418.4 keV.

[14] The neutron capture gamma rays in Table 1 tend to have high energies (several MeV). Their cross sections and intensities vary widely. The high cross sections for gamma rays from Cl make these gamma rays useful for mapping Cl abundances. The neutron capture gamma rays from H, Si, and Fe have lower cross sections but are observed with fairly high counting rates because of the high abundances of those elements. Because these neutron capture gamma rays have cross sections that only deviate slightly from the inverse of their speed, they are good for determining elemental ratios.

2.2. Nonelastic-Scattering Reactions Induced by Fast Neutrons

[15] Most gamma rays produced by fast neutrons are made by inelastic-scattering reactions, e.g., ^{28}Si(n,nγ)^{28}Si, with the gamma ray emitted from an excited level of the target nucleus. In a few cases, such as ^{16}O(n,n$\alpha\gamma$)^{12}C, the excited level is in a nucleus that is different from the target nucleus, and the interaction is usually called a nonelastic-scattering reaction. There are also a few cases where the gamma ray is from the decay of a radionuclide, such as the 6129 keV gamma ray produced by 67% of the decays of the radionuclide ^{16}N (half-life of 7 s) made by (n,p) reactions with ^{16}O. This reaction is included because it produces a 6129 keV gamma ray in the Martian atmosphere that is not Doppler broadened due to motion of the excited nucleus as it decays [*Evans et al.*, 2006] and that could interfere with measurement of the oxygen content of the Martian surface. Two reactions that can produce the 1461 keV gamma ray from ^{40}Ar are included to allow us to estimate the contributions of those reactions in the Martian atmosphere to the same energy gamma ray from the decay of ^{40}K in the Martian surface.

[16] The cross sections for making such inelastic- or nonelastic-scattering gamma rays vary. The cross sections are zero below a threshold energy, typically ~1–6 MeV for inelastic-scattering reactions and higher for other reactions. The cross sections increase rapidly above the threshold and reach a maximum a few MeV higher in energy. The cross sections then decrease with increasing energy to fairly low values above ~20 MeV. To properly calculate rates for making such gamma rays, the cross sections for each reaction as a function of energy need to be known from threshold to energies well above 20 MeV.

[17] The cross sections for making these gamma rays with fast neutrons are in worse shape than those for neutron capture reactions. Often, there have been no or only a few cross-section measurements since the detailed evaluation reported by *Reedy* [1978] and used since then by many workers. The cross sections adopted here for making some of these gamma rays were based, at least in part, on evaluations or measurements available at the National Nuclear Data Center (NNDC) of the Brookhaven National Laboratory. For many cases, the cross sections were based on prompt gamma ray measurements done at the Los Alamos Neutron Science Center (LANSCE) using a target many meters from a pulsed spallation-neutron source. The energy of the neutrons is determined by the time that it took the neutron to travel from the source to the target [*Nelson et al.*, 1991; *Bernstein et al.*, 2001]. Because measurements have been reported for only a few of the targets irradiated at LANSCE, one of us (D.M.D.) has analyzed the spectra for several irradiated targets to get cross sections. These cross sections usually are in good agreement with published cross sections, with many of these cross sections below ~20 MeV

within ~10–20% of those adopted by *Reedy* [1978]. The LANSCE data above 20 MeV are often the only extensive cross-section measurements for such neutron energies. For Mg, Al, Si, Ca, and Fe, the LANSCE data are in fair agreement with measurements made with quasi-monoenergetic neutrons for six energies from 6.5 to 64.5 MeV (C. M. Castaneda et al., Gamma-ray production cross sections from the bombardment of Mg, Al, Si, Ca and Fe with medium energy neutrons, submitted to *Nuclear Instruments and Methods in Physics Research, Section B*, 2006). The cross sections for energies above ~20 MeV are not as important as those at lower energies because most gamma rays are produced at the lower energies.

[18] Cross sections for some reactions, such as $^{16}O(n,n\gamma)^{16}O$ and $^{16}O(n,p)^{16}N$, have narrow strong peaks below ~14 MeV that span less than ~1 MeV. In the adopted cross sections, these narrow peaks were averaged over several MeV with little loss of information and with negligible effects on the final calculated production rates.

[19] The cross sections for the 4438 keV gamma ray from $^{12}C(n,n\gamma)^{12}C$, the 1368.6 keV gamma ray from $^{24}Mg(n,n\gamma)^{24}Mg$, the 1779.0 keV gamma ray from $^{28}Si(n,n\gamma)^{28}Si$, the 3736.5 keV gamma ray from $^{40}Ca(n,n\gamma)^{40}Ca$, and the 846.8 and 1238.3 keV gamma rays from $^{56}Fe(n,n\gamma)^{56}Fe$ were based on our newly analyzed LANSCE data and generally agreed well with results in the literature. The cross sections for the prompt gamma rays at 6128.6 (from excited ^{16}O), 5269.2 (excited ^{15}N), and 4438.0 (from excited ^{12}C) were based on the measurements at LANSCE of *Nelson et al.* [2001]. The new cross sections for the $^{16}O(n,n\gamma)^{16}O$ reaction making the 6129 keV gamma ray are ~50% higher than those of *Reedy* [1978]. The cross sections for the $^{16}O(n,p)^{16}N$ reaction were taken from evaluations available at the NNDC and are not very different from the set adopted by *Reedy* [1978] (as there have been very few measurements since then). The cross sections for the 1014.4 and 2211 keV gamma rays from $^{27}Al(n,n\gamma)^{27}Al$ were based on the new LANSCE cross sections, which agree well with most literature values. We did not use the Al cross sections of *Pavlik et al.* [1998], which are much higher than our LANSCE results and other measurements. The cross sections for the 2230 keV gamma ray from $^{32}S(n,n\gamma)^{32}S$ were based on the new LANSCE results and include both the 2230.1 keV gamma ray from the first excited level of ^{32}S and the 2228.5 keV from the 4458.9 keV level of ^{32}S. The uncertainties of these cross sections below about 20 MeV are estimated to be ~20%, based on the measurements and the agreement among various measurements.

[20] There are almost no measurements of cross sections for the 1460.8 keV gamma ray from the $^{40}Ar(n,n\gamma)^{40}Ar$ reaction, so our adopted values were based on some old evaluations at NNDC, which are not very different from the cross sections adopted for this gamma ray by *Reedy* [1978]. We also estimated cross sections for the $^{40}Ar(n,p)^{40}Cl$ reaction based on three measurements at 14–15 MeV that are archived at NNDC, the reaction threshold (6.9 MeV), and the shape for similar (n,p) reactions. The decay of ^{40}Cl produces the 1460.8 keV gamma ray 80% of the time, which is the only narrow 1460.8 keV gamma ray made in the Martian atmosphere as the prompt gamma ray from ^{40}Ar is Doppler broadened. The cross sections for the two reactions making the 1460.8 keV gamma ray probably have uncertainties greater than 20%.

[21] The gamma rays made by fast neutrons reported here are given in Table 2 along with the threshold energy for each of the reactions, the highest cross section, and the energy of this maximum cross section (or the energies if the highest cross section was for a range of energies). The adopted cross sections as a function of energy are included in the auxiliary material.[1] The inelastic-scattering cross sections for ^{12}C, ^{24}Mg, ^{28}Si, ^{32}S, ^{40}Ar, and ^{56}Fe are fairly large. However, of these gamma rays, we are using for elemental analyses only the 1779 keV gamma ray of ^{28}Si routinely and the 2230 keV gamma ray of ^{32}S occasionally. The 4438 keV gamma ray for ^{12}C is very broad, and the 847 keV gamma ray of ^{56}Fe is among a series of peaks and features that make it hard to have its peak area determined [*Evans et al.*, 2006]. Of the fast neutron reactions with smaller cross sections, we are occasionally using the 6129 keV gamma ray of ^{16}O, the 1014 and 2211 keV gamma rays of ^{27}Al, and the 3736.5 keV gamma ray of ^{40}Ca for elemental analyses.

3. Neutron Fluxes Calculated by the MCNPX Code

[22] The neutron fluxes used to calculate production rates were calculated using the Monte Carlo N Particle Extended (MCNPX) code [*Walters*, 1999]. MCNPX is an improved version of the LAHET Code System (LCS) used by *Masarik and Reedy* [1996] to calculate Martian gamma ray fluxes. MCNPX and LCS were mainly developed to calculate neutron production and transport in matter. Both codes have been well tested by comparing calculated production rates of cosmic-ray-produced ("cosmogenic") nuclides with observed concentrations [e.g., *Masarik and Reedy*, 1994; *Kim and Reedy*, 2003, 2004]. The basic approach used here to calculate rates for making gamma rays is the same as that used for cosmogenic nuclides, which is to use MCNPX-calculated particle fluxes with evaluated cross sections. This approach was adopted because most of the cross sections available in nuclear data libraries used by these codes are old and often very poor. A similar approach of using calculated particle fluxes and evaluated cross sections was also used by *Dagge et al.* [1991] in their study of Martian gamma ray fluxes. The MCNPX code is also used to calculate neutron fluxes for comparison with measurements by the Neutron Spectrometer (NS) [e.g., *Prettyman et al.*, 2004] and the high-energy neutron detector (HEND) [e.g., *Mitrofanov et al.*, 2004] instruments on Mars Odyssey and has been used to model gamma ray spectra measured by Lunar Prospector [e.g., *Prettyman et al.*, 2002, 2006].

[23] To calculate particle fluxes in Mars with MCNPX (or LCS), one needs to specify the nature of the incident particles and the composition and geometry of the irradiated object. Because the geometry used in MCNPX can be any combination of three-dimensional objects, the code can be used to study complicated geometries, such as the effect of rocks of various sizes in a soil of a different composition (which is common on Mars and can complicate modeling

[1] Auxiliary materials are available in the HTML. doi:10.1029/2005JE002655.

Table 2. Gamma Rays From Nonelastic-Scattering Reactions of Fast Neutrons, the Reaction Threshold Energy, and the Energies and Value of the Largest Cross Section for Making That Gamma Ray With the Target Element

Reaction	Gamma Ray Energy, keV	Threshold, MeV	Peak Cross Section, mb	Energy of Peak, MeV
$^{12}C(n,n\gamma)^{12}C$	4438.0	4.8	450.	8.1
$^{16}O(n,n\gamma)^{16}O$	6128.6	6.6	265.	7.5–9.0
$^{16}O(n,p)^{16}N$	6128.6	10.6	50.	11.5
$^{16}O(n,np\gamma)^{15}N$	5269.2	16.5	40.	27.5
$^{16}O(n,n\alpha\gamma)^{12}C$	4438.0	12.3	130.	19.
$^{24}Mg(n,n\gamma)^{24}Mg$	1368.6	1.4	600.	2.5–6.0
$^{27}Al(n,n\gamma)^{27}Al$	1014.4	1.1	220.	2.5–6.7
$^{27}Al(n,n\gamma)^{27}Al$	2211.	2.25	210.	7.0–9.5
$^{28}Si(n,n\gamma)^{28}Si$	1779.0	1.8	770.	4.5–6.0
$^{32}S(n,n\gamma)^{32}S$	2230.1	2.3	440.	6.7–10.0
$^{40}Ar(n,n\gamma)^{40}Ar$	1460.8	1.5	800.	3.–10.
$^{40}Ar(n,p)^{40}Cl$	1460.8	8.0	20.	14.5
$^{40}Ca(n,n\gamma)^{40}Ca$	3736.5	3.8	130.	7.0
$^{56}Fe(n,n\gamma)^{56}Fe$	846.8	0.9	1150.	6.
$^{56}Fe(n,n\gamma)^{56}Fe$	1238.3	2.1	475.	16.5

gamma ray fluxes [*Squyres and Evans*, 1992]). One also needs to select among the many options in the code. The inputs are discussed below.

3.1. Geometry and Composition Used for Mars

[24] The geometry used for our model of Mars was a series of concentric spherical shells. The outermost sphere had a radius of 3801 km, the radius of the Mars Odyssey spacecraft's orbit from the center of Mars (411 km above the Martian surface). The source of cosmic ray protons was on this surface directed inward with a cosine distribution, the option in MCNPX used by those studying cosmic ray interactions. This source causes the proton flux to be isotropic and equal at any point inside the sphere absent of any material.

[25] The Martian atmosphere was divided into 20 layers with 5% of the atmosphere in each layer. The scale height of the atmosphere was taken to be 10.8 km. The distances of the boundaries of these layers from the surface in the Martian atmosphere were very similar to those of *Masarik and Reedy* [1996]. These correct distances and atmospheric densities are needed to properly account for decay of pions to muons in the atmosphere [cf. *Prettyman et al.*, 2004]. The atmosphere's composition (in wt %) was 26.41% C, 1.74% N, 70.38% O, and 1.47% Ar.

[26] The radius of the Martian surface was fixed at 3390 km. Below the Martian surface, Mars was divided into many layers, with the layers thin (0.5 cm) in the top 20 cm of the surface, the depths from which most gamma rays escape into the atmosphere. Layers were progressively thicker for greater depths. The densities of these layers were 1.0 g/cm^3. (The use of the actual density, which is not well known, is not critical as long as the value used is not too different from the actual one [*Masarik and Reedy*, 1996]). The layers extended to depths well below the source of gamma rays escaping from Mars. The compositions of the layers can be varied, but usually the composition used for all depths was one that was based on measurements at Mars Pathfinder [e.g., *Wänke et al.*, 2001] with variable amounts of H_2O added. For the case of 3% water in the surface used for the calculations below, the weight percentages of the major elements were H (0.34%), O (45.34%), Na (1.76%), Mg (4.77%), Al (5.04%), Si (21.7%), S (2.0%), Cl (0.54%), K (0.51%), Ca (4.77%), Ti (0.50%), and Fe (11.76%). Minor and trace elements were about 1%. The strongly neutron-absorbing elements Sm and Gd were 3 and 4 ppm, respectively. For our calculations, the composition was assumed to be uniform with depth. The gamma ray data show no indications of layering in the middle latitudes being studied here on the ~500 km scale of the GRS footprint for either H (Boynton et al., submitted manuscript, 2006) or Cl [*Keller et al.*, 2006]. Layering on a few square meters scale could affect local neutron and gamma ray fluxes. However, the global extent of layering on Mars is not known, and much of Mars is heavily mantled to depths of many meters (H. E. Newsom et al., Geochemistry of Martian soil and bedrock in mantled and less mantled terrains with gamma ray data from Mars Odyssey, submitted to *Journal of Geophysical Research*, 2006) and probably does not have much layering. Adjacent regions within a footprint probably have different depths in which an element is enhanced, which would tend to cancel effects of layering.

3.2. Incident Galactic Cosmic Ray Particles

[27] As with our previous calculations, the incident galactic cosmic ray (GCR) particles are assumed to be protons only. Although the galactic cosmic rays contain ~13% nuclei of ^{4}He and 1% heavier nuclei, these other particles are ignored for two main reasons. One reason is that codes like MCNPX are not well tested for the interactions of heavier particles. The main reason that these heavier particles are ignored is that previous studies [e.g., *Masarik and Reedy*, 1994] have shown that increasing the flux of GCR protons by about 40% does a good job of calculating the final distributions of neutrons and other particles in matter.

[28] The GCR flux varies with time in the solar system, with the lowest fluxes at time of maximum solar activity (such as when Mars Odyssey arrived at Mars) and increases until the Sun is least active. The spectral shape used for GCR protons is that of *Masarik and Reedy* [1994] and is the same as used by most others [e.g., *Masarik and Reedy*, 1996; *Kim and Reedy*, 2004]. We divided the incident GCR protons into 26 energy bins, which went from 30 MeV up to 30 GeV, and we included those few GCR protons with higher energies in the last (20–30 GeV) bin. The spectrum of GCR protons averaged over several solar cycles [*Masarik and Reedy*, 1994] was used.

[29] This description of the incident GCR protons has been well tested with cosmogenic nuclides in meteorites [*Kim and Reedy*, 2004] and the Moon [*Kim and Reedy*, 2003]. It is the same used for calculating Martian gamma ray fluxes by *Masarik and Reedy* [1996].

3.3. Parameters Used for the MCNPX Calculations

[30] We used version 2.5e of MCNPX. The cascade-exciton model (CEM 2000) model [*Mashnik and Sierk*, 2002] was used to model the interaction of high-energy particles. The CEM 2000 model gives results that are not very different from using the default physics model (Bertini) in MCNPX [*Kim and Reedy*, 2004]. The production and transport of protons, neutrons, and pions were considered.

Pions are important particles made by high-energy GCR particles in matter and can make many neutrons. Other options in MCNPX were the default ones. These options are very similar to those used by *Prettyman et al.* [2004].

[31] For the cross sections needed by MCNPX in calculating the final distribution of neutrons and protons, we mainly used the 60c set in the MCNPXDATA DLC-205 library provided with MCNPX from the Oak Ridge National Laboratory's Radiation Safety Information Computational Center. These options and libraries for MCNPX are the same as used for previous tests with cosmogenic nuclides [e.g., *Kim and Reedy*, 2003, 2004].

[32] The results that were determined by MCNPX for each layer were the fluxes of neutrons for a series of energy bins, including a thermal bin (up to 0.3 eV), an epithermal bin (0.3 eV to 0.5 MeV), and many energy bins for fast neutrons. Energy bins for fast neutrons were 1 MeV wide below 20 MeV and got progressively larger at higher energies. A special neutron energy bin from 2 to 35 MeV was also used as the calculated neutron fluxes in that energy bin track very well production rates for the 1779 keV gamma ray from silicon for a wide range of scenarios.

[33] The Monte Carlo calculations in MCNPX use random numbers to select among a huge number of options, such as the energy and direction of the incident particle, where it first interacted, and the products of this interaction. We used enough incident protons (usually ~100,000) to get statistics at the level of about 1% or better for all of the energies and depths of interest.

4. Calculated Rates for Producing Gamma Rays

[34] The rates for making gamma rays for a composition were calculated using the nuclear data described above and the MCNPX-calculated neutron fluxes for the layers of interest. The composition was that specified in MCNPX for that layer, because fluxes can change with composition. For the work reported here, the compositions given earlier for the Martian surface and atmosphere were always used. Production of nonelastic-scattering gamma rays by protons was ignored because the fluxes of fast neutrons below about 50 MeV (the energy below which almost all gamma rays are made) are ~2–3 orders of magnitude higher than those of protons of the same energy [e.g., *Masarik and Reedy*, 1994].

4.1. Rates for Neutron Capture Reactions

[35] The relative rates for the neutron capture reactions in Table 1 (or any other neutron capture reaction) were determined using the fluxes for our thermal neutron energy bin (0–0.3 eV) calculated by MCNPX and the thermal cross sections for that reaction. Because the fractional contribution for capture by neutrons with energies >0.3 eV is the same for all elements studied here, we did not make any corrections for gamma rays made by neutrons with energies >0.3 eV.

4.2. Rates for Nonelastic-Scattering Reactions by Fast Neutrons

[36] The rates for making gamma rays with fast neutrons were calculated by numerically summing the product of the evaluated cross sections and the MCNPX-calculated neutron fluxes for the neutron fluxes above the threshold for each reaction. This is the same procedure used for most cosmogenic nuclides [e.g., *Masarik and Reedy*, 1994; *Kim and Reedy*, 2004]. This procedure has been shown to give results within 1% of exact calculations for gamma ray fluxes [*Reedy et al.*, 1973]. These procedures were done using software written for and tested with results for cosmogenic nuclides [e.g., *Kim and Reedy*, 2003, 2004]. Because of the small widths of the energy bins, the uncertainty in doing such a numerical integration is comparable to the uncertainties in the calculated neutron fluxes and much lower than the uncertainties in the cross sections.

4.3. Calculated Production Rates

[37] Figure 1 shows the calculated relative production rate profiles for making the 1779 keV gamma ray by the $^{28}Si(n,n\gamma)^{28}Si$ reaction and the sum for the 7631 and 7645 keV gamma rays (called collectively as 7638 keV) made by the $^{56}Fe(n,\gamma)^{57}Fe$ reaction for the case of a 16 g/cm^2 thick atmosphere and a surface of Mars Pathfinder composition with 3% water. The shapes of these production profiles vary with the atmospheric thickness and the H (water) content of the surface [*Masarik and Reedy*, 1996]. The depths of the maximum production rates are similar to results calculated for lunar radionuclides made by similar reactions [e.g., *Kim and Reedy*, 2003]. In both cases, the peak is below the surface. The peak for neutron capture reactions is deeper than that for fast neutron reactions.

5. Calculated Gamma Ray Intensities at the Surface as a Function of Emission Angle

[38] The intensities of gamma rays escaping the Martian surface with no change in energy as a function of the angle at the surface relative to the normal were calculated using the production rates calculated for the many depths near the surface and attenuation coefficients for each gamma ray. Total attenuation coefficients without coherent scattering were taken from the XCOM database of the National Institute of Standards and Technology (http://physics.nist.gov/PhysRefData/Xcom/Text/XCOM.html), which is based on earlier work [e.g., *Hubbell*, 1982]. Coherent scattering is when a gamma ray scatters from a bound electron without changing that electron's atomic level and thus only negligibly changes the gamma ray's energy and direction [*Masarik and Reedy*, 1996]. At the energies involved here (above ~1 MeV), coherent cross sections are 1% or less of the total cross section for gamma ray attenuation. These attenuation coefficients are well known, and the ones used here were within about 1% of those used by *Masarik and Reedy* [1996] for gamma ray transport.

[39] This intensity of each gamma ray of interest is calculated at the surface of Mars at 21 discrete values (from 0 to 1 in steps of 0.05) of the cosine of the emission angle relative to the surface's normal. This calculation is done by summing over all layers the gamma ray production rate multiplied by the attenuation factor for the path length from the median depth in that layer to the surface for that angle. Production rates for gamma rays in the Martian surface first increase with increasing depth in the Martian surface, reach a maximum within 150 g/cm^2 of the surface, and then decrease at greater depths. The intensity of a gamma ray as a function of emission angle depends on the gamma ray's

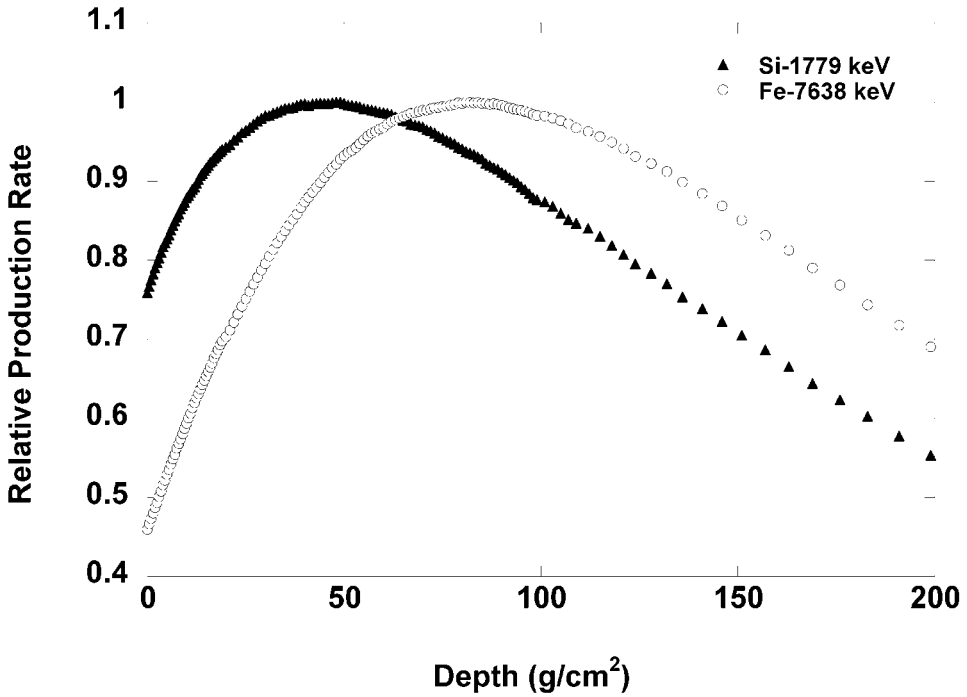

Figure 1. Calculated relative production rate profiles for making the 1779 keV gamma ray by the $^{28}Si(n,n\gamma)^{28}Si$ reaction and the sum for the 7631 and 7645 keV gamma rays made by the $^{56}Fe(n,\gamma)^{57}Fe$ reaction for the case of a 16 g/cm^2 thick atmosphere and a surface of Mars Pathfinder composition with 3% water. The very slight discontinuities at 100 g/cm^2 and other depths are results of a change in the energy bin size and the way we plotted the data.

production profile and the magnitude of its attenuation coefficient in the surface. For the reactions used here, the increase with production with greater depths results in the gamma ray intensity being the highest for emission normal to the surface and the lowest for emission at angles near perpendicular to the normal.

[40] Examples of gamma ray intensities at the Martian surface as a function of angle are shown in Figure 2 for the two gamma rays in Figure 1. Also shown is the intensity as a function of angle for the 1461 keV gamma ray of ^{40}K with the potassium assumed uniform with depth. Figure 2a shows the angular-dependent intensity of gamma rays escaping per unit area on the surface (technically called a current). Elemental concentrations in Mars are determined using the measured gamma ray count rates and forward calculations of the count rates expected for a nominal concentration. Details on these forward calculations are given by Boynton et al. (submitted manuscript, 2006) and involve the gamma ray intensities calculated here, attenuation by the atmosphere, and the detector's efficiency for counting that gamma ray. Because our forward calculations are done per unit surface area, the values in Figure 2a are used in these calculations. Figure 2b shows the fluxes per unit area perpendicular to the gamma rays' direction, which were calculated by dividing the currents (shown in Figure 2a) by the cosine of the emission angle. At the Martian surface, Figure 2b shows that the flux of 1461 keV gamma rays from the decay of ^{40}K are isotropic but that the gamma rays made by inelastic-scattering and capture reactions induced by neutrons have reduced fluxes for angles away from the normal. This effect was discussed for the Moon by *Reedy et al.* [1973] and is due to the increase in production with depth mentioned above. The values at the top of the atmosphere show the effects of attenuation through the Martian atmosphere on these gamma rays, which are to reduce considerably the flux of gamma rays and to slightly improve the spatial resolution [cf. *Boynton et al.*, 2004].

6. Summary

[41] Because the thickness of the Martian atmosphere and occasionally the nature of the surface (e.g., seasonal CO_2 layers) vary with both time and location, a series of forward calculations are done of the gamma ray counting rates expected for each 20 second accumulation by the Mars Odyssey gamma ray spectrometer. These forward calculations are needed to obtain elemental abundances from measured gamma ray counting rates. The intensity per unit surface area of each gamma ray as a function of angle at the surface is needed for these forward calculations (Boynton et al., submitted manuscript, 2006). The nuclear data and calculational procedures for determining these surface intensities are described above.

[42] The cross sections used for the production of many gamma rays made by both thermal ($\sim$0.025 eV) and fast (MeV) neutrons are presented in Tables 1 and 2, respectively. The cross sections for making gamma rays by the capture of thermal neutrons are well known. The adopted cross sections for the production of gamma rays by fast neutrons were evaluated using values taken from the liter-

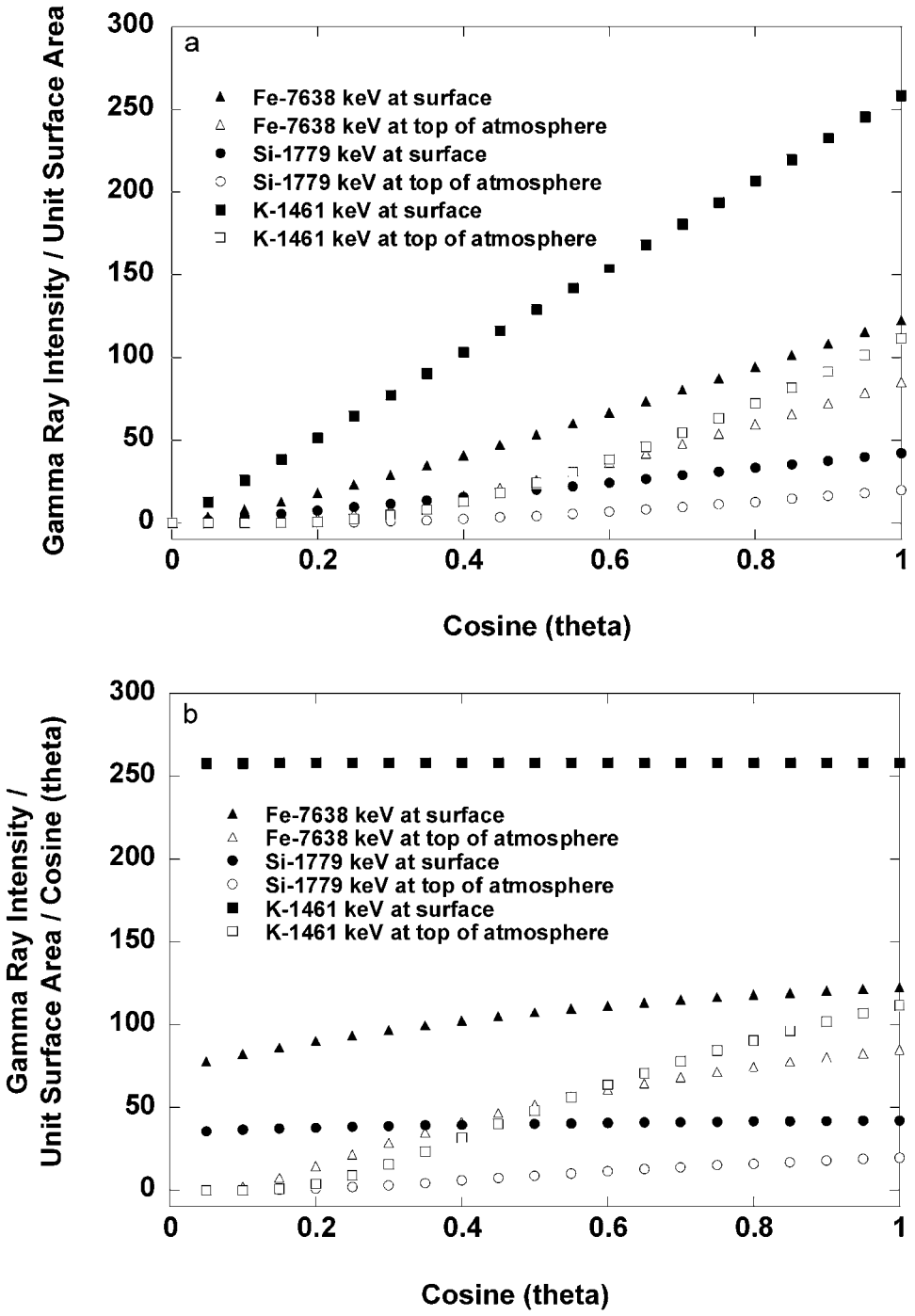

Figure 2. Relative gamma ray intensities (gamma rays/cm^2) as a function of the cosine of the angle relative to the surface's normal for three gamma rays (the Si 1779 keV and Fe 7631 + 7645, called 7638, keV gamma rays in Figure 1, and the 1461 keV gamma ray made by the natural decay of ^{40}K). Figure 2a has relative intensities both at the Martian surface and above 16 g/cm^2 of atmosphere for each gamma ray per unit area on the Martian surface. Figure 2b has the intensity from Figure 2a divided by the cosine of the angle.

ature and from unpublished measurements at the Los Alamos Neutron Scattering Center.

[43] The fluxes of fast and thermal neutrons as a function of depth in Mars for a range of atmospheric thicknesses and surface hydrogen contents were calculated using the MCNPX code. As discussed above, this code has been validated using experimental measurements of nuclides made in matter exposed to cosmic ray particles. The rates for making gamma rays were calculated using these MCNPX-calculated neutron fluxes and the adopted cross sections. Examples of these calculated production rates are shown in Figure 1 for the 1779 keV gamma ray made by

the $^{28}Si(n,n\gamma)^{28}Si$ reaction and the sum for the 7631 and 7645 keV gamma rays made by the $^{56}Fe(n,\gamma)^{57}Fe$ reaction for the case of a 16 g/cm^2 thick atmosphere and a surface of Mars Pathfinder composition with 3% water. They show an increase with depth near the surface followed by decreases with depth.

[44] The method used to calculate the intensity per unit surface area of each gamma ray for 21 emission angles at the Martian surface was presented. These intensities for a range of atmospheric thicknesses and surface compositions are critical for our forward calculations and for obtaining elemental abundances from the gamma ray measurements done by the Mars Odyssey gamma ray spectrometer. Examples are shown in Figure 2a for the two gamma rays in Figure 1 and for the 1461 keV gamma ray from the natural decay of ^{40}K. Figure 2b shows the fluxes (intensities divided by the cosine of the angle relative to the normal) of these gamma rays as a function of the cosine of the angle. Figure 2b shows the effect of the atmosphere in reducing the flux of all gamma rays for angles away from the spacecraft's nadir (''limb darkening''). At the surface, the gamma rays made in inelastic-scattering reactions are slightly limb darkened and the gamma rays made by neutron capture reactions are more strongly limb darkened. This behavior at the surface depends on the shape of the production profile, as discussed in detail by *Reedy et al.* [1973].

[45] **Acknowledgments.** This work was supported by the Mars Odyssey project. We thank Tom Prettyman and Gregg McKinney for their help in running the MCNPX code and two anonymous reviewers for their useful comments.

References

Bernstein, L. A., et al. (2001), Studying the role of nuclear structure effects in neutron-induced reactions using GEANIE at LANSCE, *Nucl. Phys. A*, *682*, 404c–414c.

Bielefeld, M. J., R. C. Reedy, A. E. Metzger, J. I. Trombka, and J. R. Arnold (1976), Surface chemistry of selected lunar regions, *Proc. Lunar Sci. Conf.*, *7th*(3), 2661–2676.

Boynton, W. V., et al. (2004), The Mars Odyssey gamma-ray spectrometer instrument suite, *Space Sci. Rev.*, *110*, 37–83.

Dagge, G., P. Dragovitsch, D. Filges, and J. Brückner (1991), Monte Carlo simulation of Martian gamma-ray spectra induced by galactic cosmic rays, *Proc. Lunar Planet. Sci. Conf.*, *21st*, 425–435.

Evans, L. G., and S. W. Squyres (1987), Investigation of Martian H_2O and CO_2 via orbital gamma ray spectroscopy, *J. Geophys. Res.*, *92*, 9153–9167.

Evans, L. G., R. D. Starr, J. Brückner, R. C. Reedy, W. V. Boynton, J. I. Trombka, J. O. Goldsten, J. Masarik, L. R. Nittler, and T. J. McCoy (2001), Elemental composition from gamma-ray spectroscopy of the NEAR-Shoemaker landing site on 433 Eros, *Meteorit. Planet. Sci.*, *36*, 1639–1660.

Evans, L. G., R. C. Reedy, R. D. Starr, K. E. Kerry, and W. V. Boynton (2006), Analysis of gamma ray spectra measured by Mars Odyssey, *J. Geophys. Res.*, doi:10.1029/2005JE002657, in press.

Firestone, R. B., Z. Revay, and G. L. Molnar (2003), New capture gamma-ray library and atlas of spectra for all elements, in *Capture Gamma-Ray Spectroscopy and Related Topics*, edited by J. Kvasil, P. Cejnar, and M. Krticka, pp. 507–513, World Sci., Hackensack, N. J.

Frankle, S. C., R. C. Reedy, and P. G. Young (2001), Improved photon-production data for thermal neutron capture in the ENDF/B-VI evaluations, *Rep. LA-13812*, 74 pp., Los Alamos Natl. Lab., Los Alamos, N. M.

Hubbell, J. H. (1982), Photon mass attenuation and energy-absorption coefficients from 1 keV to 20 MeV, *Int. J. Appl. Radiat. Isot.*, *33*, 1269–1290.

Keller, J., et al. (2006), Equatorial and midlatitude distribution of chlorine measured by Mars Odyssey GRS, *J. Geophys. Res.*, *111*, E03S08, doi:10.1029/2006JE002679. [printed *112*(E3), 2007]

Kim, K. J., and R. C. Reedy (2003), Numerical simulations of cosmogenic nuclide production rates in the Apollo 15 deep drill core, *Geochim. Cosmochim. Acta*, *67*, suppl. 1, A214.

Kim, K. J., and R. C. Reedy (2004), Production rates of cosmogenic nuclides in the Knyahinya L-chondrite, *Lunar Planet. Sci.*, *XXXV*, Abstract 1359.

Masarik, J., and R. C. Reedy (1994), Effects of bulk composition on nuclide production processes in meteorites, *Geochim. Cosmochim. Acta*, *58*, 5307–5317.

Masarik, J., and R. C. Reedy (1996), Gamma ray production and transport in Mars, *J. Geophys. Res.*, *101*, 18,891–18,912.

Mashnik, S. J., and A. J. Sierk (2002), Recent developments of the cascade-exciton model of nuclear reactions, *J. Nucl. Sci. Technol.*, *1*, suppl. 2, 720–725.

Mitrofanov, I. G., M. L. Litvak, A. S. Kozyrev, A. B. Sanin, V. I. Tret'yakov, V. Y. Grin'kov, W. V. Boynton, C. Shinohara, D. Hamara, and R. S. Saunders (2004), Soil water content on Mars as estimated from neutron measurements by the HEND instrument onboard the 2001 Mars Odyssey spacecraft, *Sol. Syst. Res.*, *38*, 253–265.

Molnar, G. L., Z. Revay, T. Belgya, and R. B. Firestone (2000), The new prompt gamma-ray catalogue for PGAA, *Appl. Radiat. Isot.*, *53*, 527–533.

Nelson, R. O., C. M. Laymon, and S. A. Wender (1991), High-resolution inelastic gamma-ray measurements with a white neutron source from 1 to 200 MeV, *Nucl. Instrum. Methods Phys. Res., Sect. B*, *56*, 451–454.

Nelson, R. O., M. B. Chadwick, A. Michaudon, and P. G. Young (2001), High-resolution measurements and calculations of photon-production cross sections for $^{16}O(n,x\gamma)$ reactions induced by neutrons with energies between 4 and 200 MeV, *Nucl. Sci. Eng.*, *138*, 105–144.

Pavlik, A., H. Hitzenberger-Schauer, H. Vonach, M. B. Chadwick, R. C. Haight, R. O. Nelson, and P. G. Young (1998), $^{27}Al(n,x\gamma)$ reactions for neutron energies from 3 to 400 MeV, *Phys. Rev. C*, *57*, 2416–2426.

Prettyman, T. H., W. C. Feldman, D. J. Lawrence, G. W. McKinney, A. B. Binder, R. C. Elphic, O. M. Gasnault, S. Maurice, and K. R. Moore (2002), Library least squares analysis of Lunar Prospector gamma ray spectra, *Lunar Planet. Sci.*, *XXXIII*, Abstract 2012.

Prettyman, T. H., et al. (2004), Composition and structure of the Martian surface at high southern latitudes from neutron spectroscopy, *J. Geophys. Res.*, *109*, E05001, doi:10.1029/2003JE002139.

Prettyman, T. H., J. J. Hagerty, R. C. Elphic, W. C. Feldman, D. J. Lawrence, G. W. McKinney, and D. T. Vaniman (2006), Elemental composition of the lunar surface: Analysis of gamma ray spectroscopy data from Lunar Prospector, *J. Geophys. Res.*, doi:10.1029/2005JE002656, in press.

Reedy, R. C. (1978), Planetary gamma-ray spectroscopy, *Proce. Lunar Planet. Sci. Conf.*, *9th*, 2961–2984.

Reedy, R. C., and S. C. Frankle (2002), Prompt gamma rays from radiative capture of thermal neutrons by elements from hydrogen through zinc, *At. Data Nucl. Data Tables*, *80*, 1–34.

Reedy, R. C., J. R. Arnold, and J. I. Trombka (1973), Expected gamma ray emission spectra from the lunar surface as a function of chemical composition, *J. Geophys. Res.*, *78*, 5847–5866.

Saunders, R. S., et al. (2004), 2001 Mars Odyssey mission summary, *Space Sci. Rev.*, *110*, 1–36.

Squyres, S. W., and L. G. Evans (1992), Effects of material mixing on planetary gamma ray spectroscopy, *J. Geophys. Res.*, *97*, 14,701–14,715.

Walters, L. S. (Ed.) (1999), MCNPX users' guide, *Doc. LA-UR-99–6058*, Los Alamos Natl. Lab., Los Alamos, N. M.

Wänke, H., J. Brückner, G. Dreibus, R. Rieder, and I. Ryabchikov (2001), Chemical composition of rocks and soils at the Pathfinder site, *Space Sci. Rev.*, *96*, 317–330.

W. V. Boynton, K. J. Kim, and R. M. S. Williams, Lunar and Planetary Laboratory, University of Arizona, Tucson, AZ 85721, USA. (wboynton@lpl.arizona.edu; kkim@lpl.arizona.edu; remo@lpl.arizona.edu)

D. M. Drake, TechSource, 1418 Luisa Street, Suite 1, Santa Fe, NM 87505, USA. (ddrake@cybermesa.com)

R. C. Reedy, Institute of Meteoritics, University of New Mexico, MSC03-2050, 200 Yale Boulevard, Albuquerque, NM 87131, USA. (rreedy@unm.edu)